

# Deep search for CO emission in the Low Surface Brightness galaxy Malin 1

J. Braine<sup>1</sup>, F. Herpin<sup>1,2</sup>, and S.J.E. Radford<sup>3</sup>

<sup>1</sup> Observatoire de Bordeaux, UMR 5804, CNRS/INSU, B.P. 89, 33270 Floirac, France

<sup>2</sup> CSIC, IEM, Departamento de Física Molecular, Serrano 121, 28006 Madrid, Spain

<sup>3</sup> National Radio Astronomy Observatory, 949 N. Cherry Ave., Tucson, AZ 85721, USA

Received 25 November 1999 / Accepted 21 January 2000

**Abstract.** A sensitive search for CO emission from the Low Surface Brightness Galaxy Malin 1 has yielded negative results. The nucleus and several positions corresponding to regions of star formation in the disk were observed in the CO(1–0) and CO(2–1) lines with no detection. Use of a “standard”  $N(\text{H}_2)/I_{\text{CO}(1-0)}$  conversion factor yields  $M_{\text{H}_2}/M_{\text{HI}} < 0.03$ . However, rather than argue that there is very little molecular gas in Malin 1, where some star formation is currently taking place, we attribute the non-detection chiefly to the low temperature of the gas. Detection of CO may be rendered still more difficult by a subsolar metallicity.

**Key words:** galaxies: abundances – galaxies: evolution – galaxies: individual: Malin 1 – galaxies: ISM – galaxies: spiral – radio lines: galaxies

## 1. Introduction

Over the last decade, it has become clear that a significant population of low surface brightness galaxies exists and that many of them are spirals. Recent reviews by Bothun et al. (1997) and Impey & Bothun (1997) suggest many galaxies escape standard techniques for creating catalogs. Up to one half of all galaxies may be found in the tail of the surface brightness distribution (Fig. 1 of McGaugh et al. 1995). Dalcanton et al. (1997) came to an even more extreme conclusion about the density of low surface brightness (LSB) galaxies:  $n = .08(H/100)^3$  galaxies  $\text{Mpc}^{-3}$  with central disk surface brightness fainter than  $\mu_0 = 23.5$  mag arcsec<sup>-2</sup>, comparable to the density of normal galaxies.

The discovery of the *very* low surface brightness spiral Malin 1 (Bothun et al. 1987) sparked interest in such objects. Malin 1 is a very massive spiral, in terms of both its gaseous and stellar content, but it is so spread out it is difficult to see. Malin 1 contains lots of atomic hydrogen,  $M_{\text{HI}} \sim 4 \cdot 10^{10} M_{\odot}$  (Pickering et al. 1997), in a nearly 100 kpc disk with a disk surface brightness extrapolated to the center of  $\mu_{0V} = 25.5$  mag arcsec<sup>-2</sup> (Impey & Bothun 1989). These sizes and masses

are for a (luminosity) distance of 250 Mpc, which corresponds to  $H_0 = 100 \text{ km s}^{-1} \text{ Mpc}^{-1}$ , so they may be considered lower bounds. While the overall color is a standard B-V=0.9, Bothun et al. also found three regions of star formation with bluer colors, B-V ~ 0.3.

Malin 1 is such a low surface brightness object that it cannot be simply an extension of the variation in standard disk surface brightness. This is important because catalogs of *normal* galaxies contain some objects of low surface brightness but nothing like Malin 1.

LSB galaxies may represent a parallel evolutionary track to high surface brightness (*i.e.* normal) spirals. The low gas surface density would inhibit star formation so disks would remain unevolved for very long times. This may not be correct. Infrequent and dispersed star formation means low metallicity and thus, no CO emission given the low temperatures likely in these disks. Observing CO(1–0) and CO(2–1) is one way to check the metallicity, although a non-detection would only constrain a combination of parameters. The detection of CO in an intergalactic molecular cloud (Brouillet et al. 1992), presumably a sort of very small tidal dwarf in the M 81 group but with no optical counterpart detected so far, shows that high surface brightness is not an absolute prerequisite for CO, at least in some circumstances. This object has since been detected in <sup>13</sup>CO and thermal dust emission (in prep.).

LSB galaxies are not IRAS sources. The non-detection of Malin 1 by IRAS at 100  $\mu\text{m}$  means that the temperature of the dust in the HI gas (no molecular gas is assumed) is  $T_{\text{dust}} \lesssim 16$  K, assuming a low but still normal metallicity and grain cross-section (Draine & Lee 1984). This is several degrees lower than typically estimated for normal spirals. The expected thermal dust continuum fluxes are below the detection thresholds for extended objects with present instruments. For  $T_{\text{dust}} \lesssim 16$  K, flux densities integrated over the whole disk of  $\lesssim 7$  mJy,  $\lesssim 30$  mJy, and  $\lesssim 0.2$  Jy are expected at 1.22 mm, 850  $\mu\text{m}$ , and 450  $\mu\text{m}$ , respectively, for the observed amount of HI gas.

Malin 1 is the best-known example of a class of galaxies – big LSB spirals, not dwarfs – that could change our views of the amount of mass in galaxies and of galaxy evolution. It is massive so the lack of metallicity can not be due to its small size (like local dwarf Irregulars) but must be caused by a lack

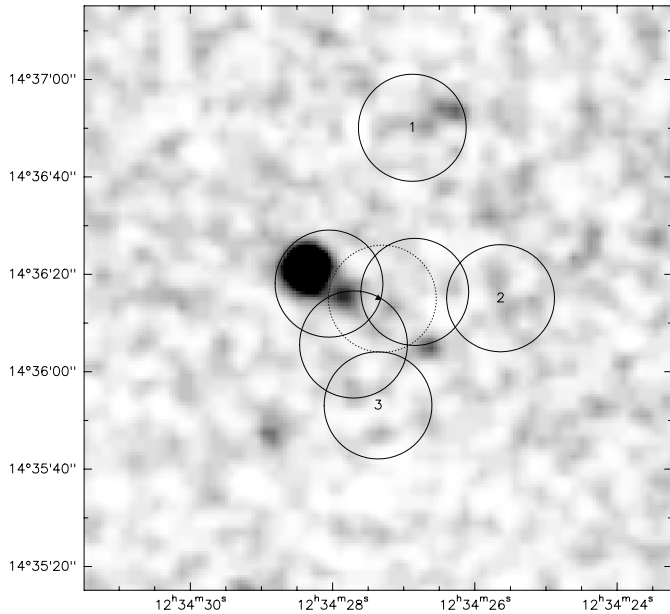


**Fig. 1.** Malin 1 region from the Digital Sky Survey. The numbers 1, 2, 3 indicate the star-forming regions with blue ( $B-V \sim 0.3$ ) colors. Coordinates are epoch B1950. The circles represent the  $22''$  beam (FWHM at 106 GHz) at the six positions. The triangle marks the position given by Bothun et al. (1987) and the dashed circle shows the region observed by Radford (1992). We confirmed the digital sky survey coordinates were indeed correct by checking the position of NGC 4571 (just below this image) with the position given in the RC3 catalog (De Vaucouleurs et al. 1991).

of star-formation, which provides both metals and a heat source for CO. It has a huge amount of HI gas so lack of neutral gas would not be the reason for a non-detection.

All this made Malin 1 an obvious target for CO searches. Impey & Bothun (1989) looked, but mistuned by 700MHz due to confusion between optical and radio conventions. Radford (1992) observed at the correct frequency but at the position given for the center in the discovery paper (Bothun et al. 1987). Unfortunately, this position is about  $17''$  (see figures) from the center or any of the star-forming regions. Here we present deep observations of the CO(1–0) and CO(2–1) lines in the right positions at the right frequency.

A search for CO(2–1) emission in LSB galaxies was recently carried out by de Blok & van der Hulst (1998). Our observations complement theirs. Where they observed three small LSB galaxies, we focus on a single large spiral, observing several positions. We observe CO(1–0) and CO(2–1) rather than just CO(2–1).

## 2. CO observations

Malin 1 was observed at the 30meter telescope operated by the Institut de Radioastronomie Millimétrique (IRAM) on Pico Veleta, Spain in May of 1998. Two single polarisation 3mm receivers were used with the two  $512 \times 1$  MHz filter banks and one 1 mm receiver was used with an autocorrelator backend. The second 1 mm receiver (230g2) could not be tuned to our

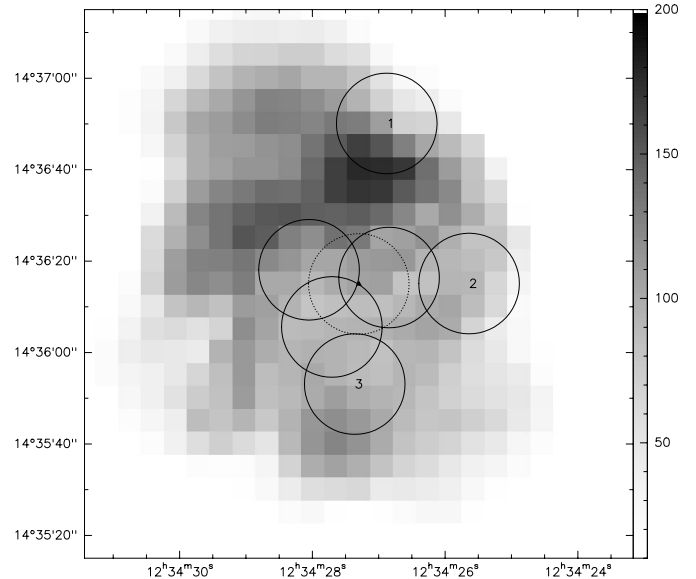


**Fig. 2.** Grey scale intensity of HI from Malin 1 (Pickering et al. 1997). The circles and other indicators are the same as in Fig. 1. The angular resolution of the HI observations is  $21''$ , roughly that of our CO(1–0) observations ( $22''$ ).

**Table 1.** Basic parameters of Malin 1. Position is center of CO map.

RA(1950)	12 34 28.05
Dec(1950)	14 36 18.1
velocity	$cz = 24733 \text{ km s}^{-1}$
redshift	$z = 0.0825$
$L_V$	$\sim 6.8 \cdot 10^{10} L_{V,\odot}$
$M_{\text{HI}}$	$4 \cdot 10^{10} M_{\odot}$
CO(1–0)	106.486 GHz
CO(2–1)	212.968 GHz

observing frequency. Pointing was checked on the strong nearby quasar 3c273 every  $\sim 90$  minutes and found accurate to within a few arcseconds. The focus was also checked by observing 3c273. Cold load calibrations were made every 4 to 15 minutes depending on atmospheric stability. System temperatures were 200 – 250 K ( $T_a^*$ ) at 106 GHz and 400 – 600 K ( $T_a^*$ ) at 213 GHz. The half-maximum beam widths of the telescope are  $22.5''$  and  $11.3''$  at our observing frequencies.

The redshifted frequencies of the CO lines is  $\nu_{\text{obs}} = \nu_{\text{rest}}/(1+z)$  where  $z$  is the “optical velocity” 24733 km/sec divided by the speed of light  $c = 299792 \text{ km/sec}$  so  $z = .08250$  and  $\nu_{\text{obs}} = 106.486 \text{ GHz}$  and  $212.968 \text{ GHz}$  for the CO(1–0) and CO(2–1) lines respectively. The 500 MHz bandwidth means the CO(1–0) observations cover the redshift interval from  $0.080 < z < 0.085$ . The frequency setting was checked by observing Orion and comparing with the spectral survey of Orion published by Turner (1989). At 106 GHz,  $^{34}\text{SO}(2_3 - 1_2)$  was observed at the band edge and  $\text{SO}(2_3 - 1_2)$  was detected in the image sideband. From this, we measured image sideband gains of 0.005 and 0.04 for the two receivers under the assumption that the  $^{34}\text{SO}/\text{SO}$  line ratio is similar in our beam as in Turner’s

**Table 2.** Observed positions in Malin 1. Offsets are with respect to the position in Table 1. The velocity (Column 4) and line width were estimated from Fig. 1 of Pickering et al. (1997).  $\Delta I_{\text{CO}}$  and  $\Delta M_{\text{H}_2}$  are  $1\sigma$ . A shallow linear baseline was subtracted from the CO(2–1) spectrum at position (-5, -12.5).

Offset arcsec	noise mK chan <sup>-1</sup>	resolution km s <sup>-1</sup>	velocity km s <sup>-1</sup>	line width km s <sup>-1</sup>	$\Delta I_{\text{CO}}$ K km s <sup>-1</sup>	$\Delta M_{\text{H}_2}$ $10^8 M_{\odot}$
<sup>12</sup> CO(1–0) results						
0,0	2.2	11.26	24733	320	0.13	3.6
-17,32	2.0	11.26	24810	120	0.07	2.0
-35,-3	2.5	11.26	24665	80	0.07	2.0
-10,-25	2.6	11.26	24630	60	0.07	1.8
-17.5,-1.7	5.0	11.26	24700	140	0.20	5.3
-5,-12.5	5.1	11.26	24630	80	0.15	4.1
total disk ( $3\sigma$ )	1.4	11.26		120	0.15	12.5
<sup>12</sup> CO(2–1) results						
0,0	7.0	7.04	24733	320	0.33	3.4
-17,32	7.4	7.04	24810	100	0.20	2.0
-35,-3	6.6	7.04	24665	60	0.14	1.4
-10,-25	6.5	7.04	24630	60	0.13	1.4
-17.5,-1.7	14	7.04	24700	100	0.38	3.8
-5,-12.5	17	7.04	24630	60	0.35	3.6

observations. Many lines were detected at 213 GHz, enabling us to confirm the frequency, but all were in the signal sideband so we must assume the nominal image gain is correct.

The observed positions in Malin 1 are the nucleus, each of the three star formation regions (Bothun et al. 1987), and two positions intermediate between the nucleus and regions 2 and 3. Figs. 1 and 2 locate our CO observations on, respectively, an optical and an HI image.

The final CO(1–0) and CO(2–1) spectra are shown in Fig. 3. The reduction process was simple: subtract any underlying continuum level (*i.e.* a zero order baseline) based on the channels outside the expected line window and take the average of all spectra for each position. All data are presented on the main beam temperature scale, assuming beam efficiencies of 0.72 and 0.48 at 106 and 213 GHz respectively.

### 3. Results and analysis

#### 3.1. CO intensities and $H_2$ masses

The velocity resolution and *rms* noise levels of the spectra are given in Table 2. The atomic and molecular gas are subject to the same gravitational potential (the slight difference in scale height is not important for our purposes here) and as such should have the same rotational velocities at the same positions. The velocity (Column 4) was estimated from Fig. 1 of Pickering et al. (1997) and we assume that any molecular gas at that position has that velocity. In the absence of strong streaming motions in spiral arms, the same argument applies for the line widths of disks. The HI line width (Column 5) was estimated by determining the span in velocities within the CO beam size from Fig. 1 of (Pickering et al. 1997), rounding up to the next contour, and adding 20 km/sec to take dispersion into account. For region 3,

we used the HI position-velocity diagram (Fig. 7) in Pickering et al. because this yielded a larger line width and for the center we assumed 320 km/sec (the entire velocity width).

We calculate CO intensities through  $\Delta I_{\text{CO}} = \sigma \sqrt{\Delta V \times \delta v}$  where  $\sigma$  is the rms noise level in Kelvins,  $\Delta V$  is the line width (Table 2 Column 5) and  $\delta v$  is the channel width (Table 2 Column 3). The corresponding  $H_2$  masses are

$$\Delta M_{\text{H}_2} = \Delta I_{\text{CO}} \times 2mp \times N(\text{H}_2) / I_{\text{CO}} \times \Omega D^2$$

where  $\Omega$  is the beamsize (assumed gaussian),  $D$  is the distance to Malin 1, and  $mp$  is the proton mass. We take a reasonable “outer disk” value of

$$N(\text{H}_2) / I_{\text{CO}(1-0)} = 2 \cdot 10^{20} \text{ cm}^{-2} (\text{K km s}^{-1})^{-1},$$

roughly valid for cool virialized molecular clouds (Dickman et al. 1986). We assume  $N(\text{H}_2) / I_{\text{CO}(2-1)} = 3 \cdot 10^{20} \text{ cm}^{-2} (\text{K km s}^{-1})^{-1}$ . The  $1\sigma$  molecular gas mass limits within the CO beams are below  $10^{-2} M_{\text{HI}}$ . Here we give  $1\sigma$  values because several measurements are available – while a single CO observation could have a  $3\sigma$  level intensity hidden by the rms noise, this cannot be true for several measurements unless unexpected strong systematic errors are present and we have no reason to believe this is the case. De Blok & van der Hulst (1998) assume a “top hat” circular beam, whereas we perform the calculations for a gaussian, and they use a higher  $N(\text{H}_2) / I_{\text{CO}(2-1)}$  factor. Using their method would decrease our estimated  $H_2$  masses (from the CO(2–1) observations) by 16%.

Finally, our disk measurements are combined to yield a best-guess  $3\sigma$  CO intensity limit which is then converted into a  $3\sigma$  limit to the molecular gas mass. Because we know the velocity of the gas at each position, we re-align the disk spectra so that any CO emission is centered around  $v = 0$  and then we average them to obtain the total CO emission coming from a synthesized

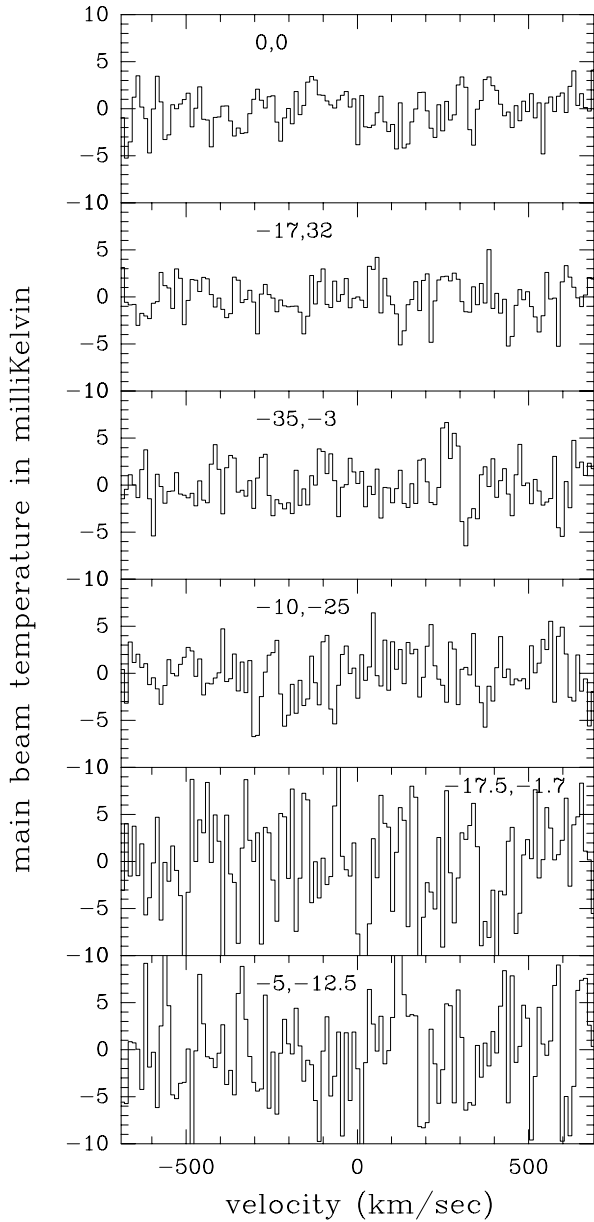


**Fig. 3.** CO(1–0) spectra of Malin 1.

beam covering the three regions of star formation and which is three times the size of the beam for an individual observation. This is given in the last row of each part of Table 2. Given that we use the greatest line width to calculate the limit, it is in fact quite conservative. We then obtain the  $3\sigma$  upper limit  $M_{\text{H}_2}/M_{\text{HI}} < 0.03$ , quite an extreme value indeed.

### 3.2. Star formation and the expected $\text{H}_2$ mass

Now we turn to the rate of star formation in Malin 1. The  $V$  band luminosity of Malin 1 is about  $7 \cdot 10^{10} L_{V,\odot}$  and about 70% of this comes from the disk, or  $5 \cdot 10^{10} L_{V,\odot}$  (Pickering et al. 1997). Assuming a lifetime of about  $10^{10}$  yr, this converts to an average SFR of about  $5 M_{\odot} \text{ yr}^{-1}$ . Similar calculations for HSB (normal) spirals yield  $1 - 5 M_{\odot} \text{ yr}^{-1}$ , in accord with other

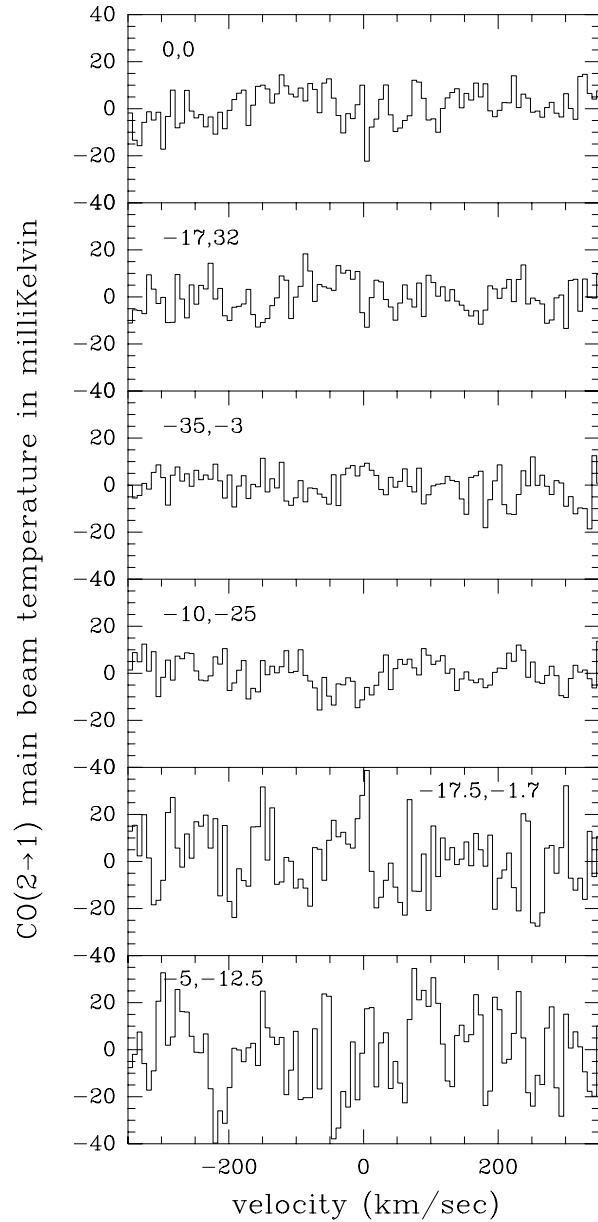


**Fig. 4.** CO(2–1) spectra of Malin 1.

means of estimating the SFR, and the estimated molecular gas masses (from CO) are  $1 - 5 \cdot 10^9 M_{\odot}$ . Such an SFR could be expected to yield an FIR luminosity of about  $2 \times 10^{10} L_{\odot}$  (Scoville & Young 1983) and generate a flux density of  $\sim 100 \text{ mJy}$  averaged over the IRAS  $100 \mu\text{m}$  band, significantly below the IRAS detection threshold.

The HI emission in Malin 1 (Fig. 2), neglecting the lowest column densities, covers slightly more than 1 square arcminute and the size of the CO(1–0) beam is about 1/6 square arcminute, so one might reasonably expect that about  $10^9 M_{\odot}$  of molecular gas should be present within the beam. Our limits are substantially below this in each case. Furthermore, if we assume that the star formation occurs in the three regions of star formation, then the  $\text{H}_2$  mass expected is a factor two higher. The “expected”  $\text{H}_2$  mass for each of the star forming regions is then 5 – 10 times

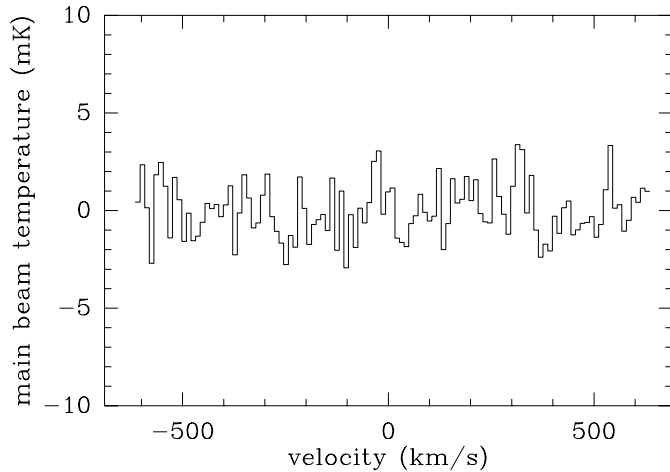


**Fig. 5.** Sum of CO(1–0) spectra of the three star-forming regions in Malin 1. The expected velocities of the CO line, assuming it is at the same velocity as the observed HI line, have all been set to zero so that CO emission from the 3 positions should add at zero velocity.

above what we obtain through standard conversion from CO to H<sub>2</sub>, as shown in Table 2.

Turning to the nucleus, with the same arguments, the V band luminosity is about  $2 \cdot 10^{10} L_{V,\odot}$ , yielding an expected H<sub>2</sub> mass of  $2 \cdot 10^9 M_{\odot}$ , well above our results. The arguments used here to estimate the SFR are likely valid for the disk, which appears to be forming stars “stochastically”, but not for the nucleus which is of much higher surface brightness and presumably formed most of its stars at an earlier epoch.

### 3.3. Why we do not detect CO

In conclusion, the CO luminosity of Malin 1 is indeed below that of a normal spiral disk with a similar star formation rate. At the scale of the individual molecular clouds, we have no reason to believe that the conversion of molecular gas into stars is more efficient in Malin 1 than in normal spirals. This reasoning implies that Malin 1 contains a “normal” (roughly  $10^9 \times \text{SFR } M_{\odot}$ ) amount of H<sub>2</sub>. Let us first note that this yields an H<sub>2</sub>/HI mass ratio of 0.1, well below what is found in normal spirals. Malin 1 is thus a spiral with a luminous bulge and a very high HI mass fraction – an unusual object on even just these criteria. The low HI surface density makes conversion to H<sub>2</sub> slow and dependent on local fluctuations. Our CO-based “limits” to the H<sub>2</sub> mass are a factor 5 or so below what is expected from the estimated SFR and this is the case for several independent positions.

*Why do we then not detect the CO?* A subsolar metallicity may be partially responsible but we expect (a) that Malin 1, because it is a giant spiral, may not have a very low metallicity and (b) that the effects of metallicity on the CO–H<sub>2</sub> conversion ratio will be much less important than in bright blue metal-deficient

galaxies. This leads us naturally to the conclusion that the gas (and dust) is quite cold, such that the CO (and dust) emission from molecular gas clouds is much less than in the disk of our galaxy. This will considerably reduce the CO emission per mass of H<sub>2</sub> and, combined with metallicity effects, could explain why we have not detected CO(1–0). Transitions higher than CO(1–0) will become rapidly much more difficult to detect. Firstly because the Rayleigh-Jeans approximation ( $\frac{h\nu}{kT} \ll 1$ ) used to convert power to antenna temperature is not fully appropriate at these frequencies and becomes less appropriate with increasing frequency. Secondly, collisional excitation of higher transitions requires higher densities, further reducing the emission if the molecular gas is, on average, less dense than in our galaxy. A further reduction in CO emission could be caused by condensation of molecules onto dust grains. There is no evidence for this at large scales but it has been observed in very dense cool clouds (Kruegel & Chini 1994). Whether such a process could be important in Malin 1 is unknown. The lack of CO could also be explained if the star formation recently stopped in Malin 1. We regard this as highly improbable because galactic disks are dominated by continuous star formation rather than bursts and this should be particularly true for these isolated systems.

We attribute the low CO luminosity of Malin 1 to the low temperature of the molecular gas *possibly* compounded by a subsolar metallicity and/or condensation of molecules onto dust grains. Further attempts to detect CO emission in low-brightness objects should be carried out in (at least) the CO(1–0) transition.

*Acknowledgements.* We thank Jacqueline van Gorkom for the use of the Pickering et al. (1997) HI column density map.

### References

- Bothun G., Impey C., McGaugh S., 1997, PASP 109, 745
- Bothun G. D., Impey C. D., Malin D. F., Mould J. R., 1987, AJ 94, 23
- Brouillet N., Henkel C., Baudry A., 1992, A&A 262, L5
- Dalcanton J. J., Spergel D. N., Gunn J. E., Schmidt M., Schneider D. P., 1997, AJ 114, 635
- De Blok W. J. G., Van Der Hulst J. M., 1998, A&A 336, 49
- De Vaucouleurs G., De Vaucouleurs A., Corwin J. R., Buta R. J., Paturel G., Fouque P., 1991, in Third reference catalogue of bright galaxies (1991)
- Dickman R. L., Snell R. L., Schloerb F. P., 1986, ApJ 309, 326
- Draine B. T., Lee H. M., 1984, ApJ 285, 89
- Impey C., Bothun G., 1989, ApJ 341, 89
- Impey C., Bothun G., 1997, ARA&A 35, 267
- Kruegel E., Chini R., 1994, A&A 287, 947
- McGaugh S. S., Bothun G. D., Schombert J. M., 1995, AJ 110, 573
- Pickering T. E., Impey C. D., Van Gorkom J. H., Bothun G. D., 1997, AJ 114, 1858
- Radford S., 1992, A&A 262, 13
- Scoville N., Young J. S., 1983, ApJ 265, 148
- Turner B. E., 1989, ApJS 70, 539